

Effect of Electrochemical Hydrogen Loading on the Photoelectrochemical Properties of Plasma-Grown In_2O_3

Lynn C. Schumacher*

Ontario Hydro Research Division, Toronto, Ontario, Canada M8Z 5S4

Michael J. Dignam*

Department of Chemistry, University of Toronto, Toronto, Ontario, Canada M5S 1A1

In two previous publications (1, 2) it has been shown that thermal oxidation of liquid indium metal droplets gives rise to hollow, hemispherical In_2O_3 structures which exhibit maximum quantum efficiencies of $\approx 90\%$ at 310 nm. Oxide films of the same mean thickness, grown in essentially the same way except that they were exposed to the oxygen plasma during oxidation gave maximum quantum efficiencies of $\approx 40\%$; these films being referred to as plasma oxidized In_2O_3 . On the other hand, uniform, flat films of In_2O_3 grown by reactive sputter deposition from an indium metal target in a 100% O_2 plasma, exhibited maximum quantum efficiencies of $\approx 18\%$ at 290 nm. The source of the vast improvement of the rough thermally grown films over the flat sputter-deposited films was shown to be comprised of two contributions, one based on geometry and the other related to an improvement in the solid-state properties of the former over the latter. While the plasma oxidized films have the same geometry as the thermally grown films, they were exposed to the oxygen plasma for ≈ 2 min during oxide growth, hence they would be expected to suffer impact damage as well as having a thin sputtered In_2O_3 film coating the hemispherical oxide structures. This was cited as the reason for the poorer photoanodic response of the plasma grown films compared to those thermally grown. Based on this result it was estimated that geometry and improved solid-state properties were each responsible for $\approx 50\%$ of the improvement of the rough thermally grown films over the flat reactively sputtered oxide films. In this note we provide direct evidence confirming that half of the improvement of the thermally grown films over the reactively sputtered films is due to improved solid-state properties.

In previous studies of electrochemical hydrogen loading of reactively sputtered TiO_2 films it was shown that a significant but temporary improvement in the photoanodic response could be affected by the electrochemical uptake of hydrogen (3). This present study was undertaken to see if a similar result could be obtained with In_2O_3 formed by reactive sputter deposition and by thermal and plasma oxidation of liquid indium metal droplets. Film fabrication methods and photoelectrochemical characterization techniques have been discussed at length previously (1, 2). For these studies, the oxide films were electrochemically loaded with hydrogen by biasing the electrodes at -1.50V (SCE) in 0.10M NaOH. Once the electrode was so biased, it began immediately to change color from light to dark black. This procedure was followed for all oxide films grown on conducting indium tin oxide (ITO). Once a uniform black film was obtained, the electrode was then anodically biased between -0.6 and 1.0V (SCE).

The white light photoresponse of a flat reactively sputtered film of In_2O_3 shown in Fig. 1, curve 1, did not change at all following hydrogen loading. The white light response of the rough plasma grown film did however change substantially, almost by a factor of two as comparison of curve 3 (after H_2 loading) to curve 2 (before H_2 loading) clearly demonstrates. The white light response of the H_2 loaded plasma-grown film approached that of the thermally grown In_2O_3 films, see for example Ref. (1). These latter films exhibited no improvement in photoresponse after H_2 loading. The quantum efficiency plots of Fig. 2 are for the

electrodes of Fig. 1, with the plasma-grown film showing significant improvement over the entire wavelength region. The indirect and direct bandgaps of the plasma grown In_2O_3 film did not change as a result of H_2 loading as shown by Fig. 3a and b. However the doping density of the plasma-grown films underwent substantial change with hydrogen loading leading to a 10^2 - 10^3 increase in the product KN_d (compare Fig. 4 and 5). On the other hand, the doping density of the reactively sputtered In_2O_3 film increased by a factor of 10 upon hydrogen loading (see Fig. 6).

Continuous potential cycling of the hydrogen loaded plasma grown films between -1.0 and 1.0V (SCE) for 12h had no deleterious effect on the improved photoanodic behavior nor could the hydrogen be anodically stripped out. The uptake of hydrogen is therefore irreversible, in contrast to the situation with sputtered TiO_2 films where the hydrogen could be driven out at high anodic potentials (3). Attempts to incorporate hydrogen into the oxide during lattice growth by depositing indium in an argon-hydrogen mixture followed by plasma or thermal oxidation resulted in bluish colored, metallic, incompletely oxidized films.

The improvement in photoresponse of the plasma grown films accompanying H_2 loading is clearly not due, even in part, to a modification or change in the optical or dielectric properties of the oxide since neither the reactively sputtered or thermally grown films showed any photoanodic improvement upon H_2 loading. This is further supported by the bandgap plots of Fig. 3 which show the same bandgaps before and after H_2 uptake. The source of the improvement must therefore be a reduction in defect or recombination centers present in the plasma grown films while absent in the thermally grown oxide. Interestingly, while the photoanodic behavior of the plasma oxidized films undergo a dramatic improvement upon hydrogen uptake, both the reactively sputtered and thermally grown films do not. That the thermally grown films do not improve is probably because they possess already the opti-

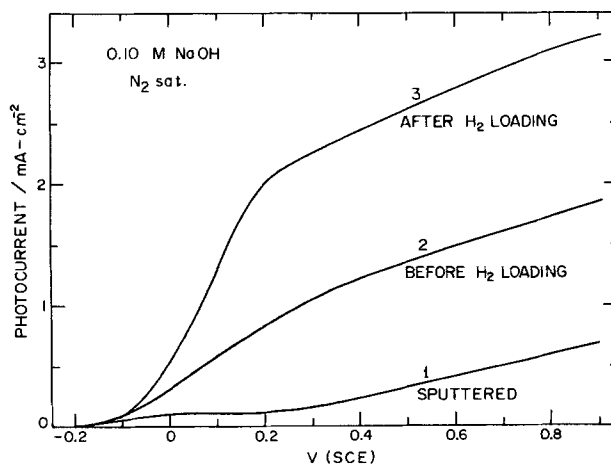


Fig. 1. White light photoresponse for: curve 1, uniform flat reactively sputtered In_2O_3 films $\approx 2000\text{\AA}$ in thickness; curve 2, a colloidal rough In_2O_3 film of mean thickness $\approx 1700\text{\AA}$ grown by plasma oxidation of liquid indium metal droplets; curve 3, same films as curve 2 but after electrochemical hydrogen loading.

* Electrochemical Society Active Member.

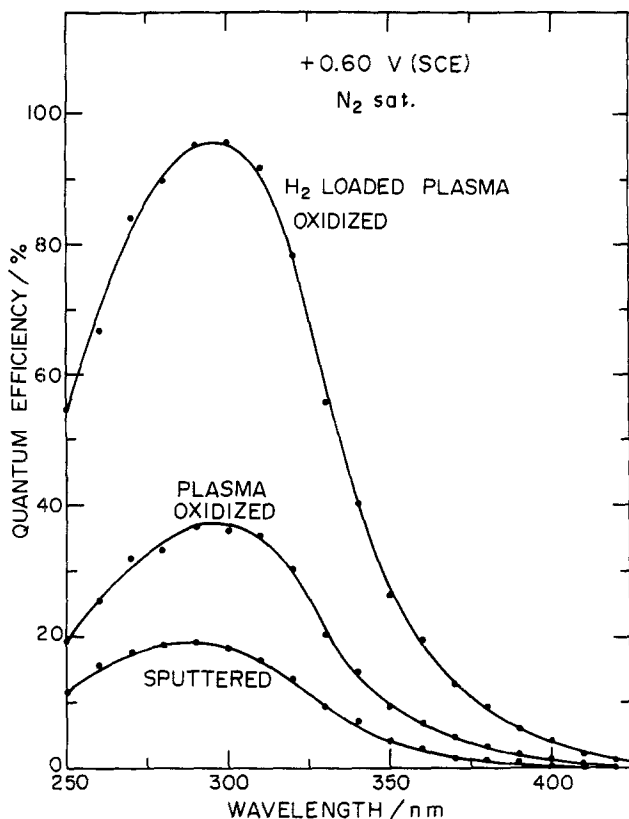


Fig. 2. Quantum efficiency plots for the electrodes of Fig. 1, those for the reactively sputtered and plasma oxidized film are from Ref. (2).

mum solid-state properties that cannot be improved upon. However, the reactively sputtered films show no improvement at all, this in spite of the fact that they will most likely possess the highest concentration of lattice defects, this being supported by the nonlinear Mott-Schottky plots and the higher doping densities (compare Fig. 4 and 6). Comparison of the doping densities of these two films after the electrochemical uptake of hydrogen reveals less hydrogen was taken up by the sputtered films. The structure type to which In_2O_3 belongs is the C-rare earth oxide. Oxides in this class crystallize in a fluor spar type lattice (CaF_2) characterized by vacancies in the anion sublattice. This suggests that In_2O_3 should be able to take up hydrogen readily. There are several possible reasons why the plasma-grown films are taking up more hydrogen than the reactively sputtered films. First, being hollow collapsed

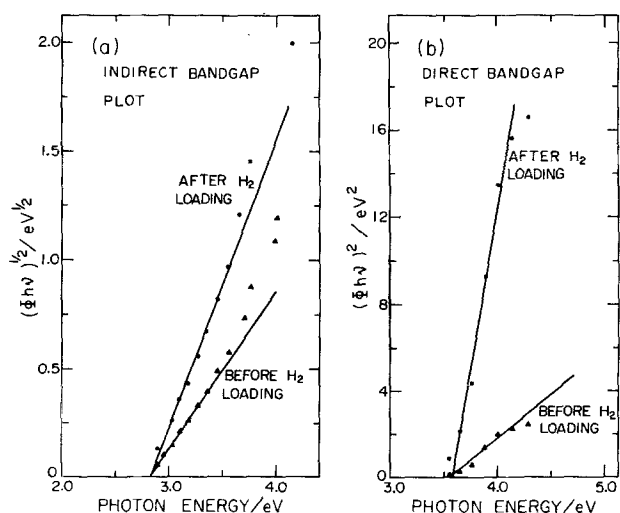


Fig. 3. (a) Indirect bandgap plot for the plasma grown In_2O_3 film, before and after electrochemical hydrogen loading. (b) Direct bandgap plot for the plasma grown films, before and after hydrogen loading.

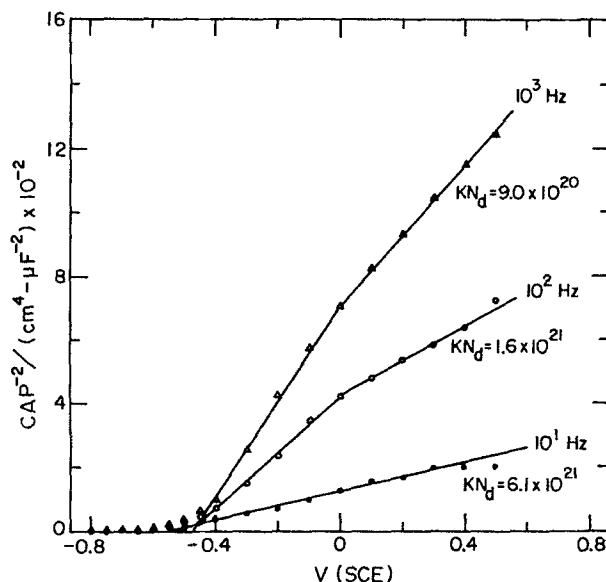


Fig. 4. Mott-Schottky plots of the plasma oxidized In_2O_3 before electrochemical hydrogen loading.

hemispherical structures [see Ref. (2)], these films have higher surface areas than the sputtered films. Second, as the XRD spectra of Fig. 7 show, there are strong orientation differences between the two differently grown oxides. This is to be expected since the growth mechanisms are so radically different, with the flat reactively sputtered films being grown one atomic layer at a time while the plasma (and thermally) grown films grow radially by metal migration through the oxide crust. Besides strong orientation effects, slight differences in film density, In/O ratio and the defect structure, type and concentration of defects will exist. Since incorporation of tin from the underlying ITO layer into the reactively sputtered In_2O_3 will occur but is not expected in the plasma-grown films, this will also result in defect differences between the two types of film. That the hydrogen is having no beneficial effect on the photoanodic properties of the sputtered films is probably due to the hydrogen having much less impact in a much more defective structure due to grain boundaries, point defects brought about by impact damage and impurity diffusion from the underlying ITO substrate.

Several conclusions can be drawn from these studies of electrochemical hydrogen loading of In_2O_3 formed by reac-

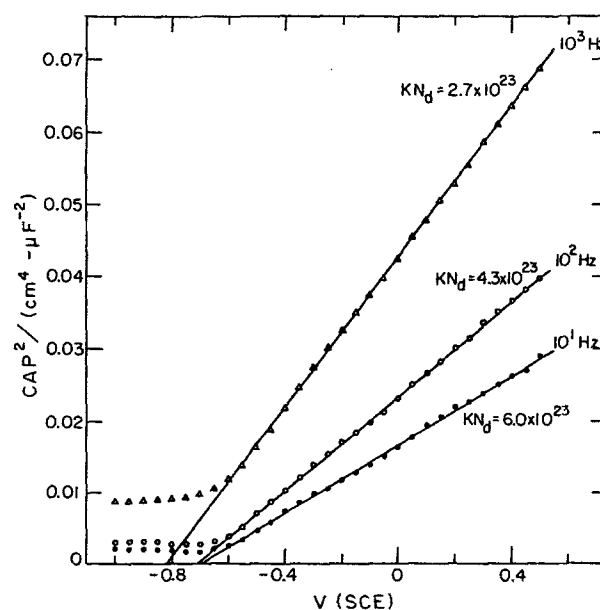


Fig. 5. Mott-Schottky plots for the film of Fig. 4 after electrochemical hydrogen loading.

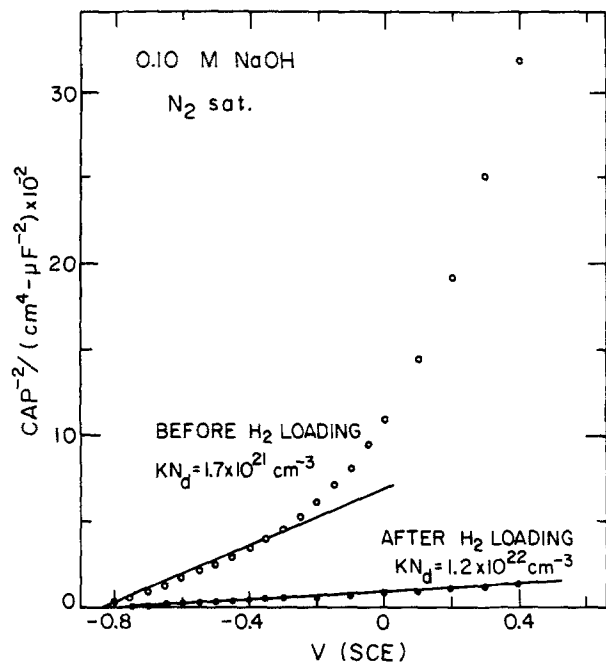


Fig. 6. Mott-Schottky plots of the flat reactively sputtered In_2O_3 film at 10^3 Hz before and after electrochemical hydrogen loading.

tive sputtering, plasma and thermal oxidation of liquid indium metal films. First, the poorer photoanodic behavior of the plasma-grown oxide relative to the thermally grown oxide is due to a higher concentration of lattice defects or recombination centers in the former, no doubt introduced by bombardment of the oxide by the oxygen ions. That hydrogen uptake by the plasma-grown oxides reproducibly leads to the same efficiencies as the thermally grown films supports the previous estimate that approximately half the improvement of the thermally grown In_2O_3 over the flat sputtered films is due to superior solid-state properties of the former over the latter. Second, the mechanism of lattice growth is having a significant impact on the ability of the oxide to electrochemically take up hydrogen.

Manuscript received Jan. 27, 1989.

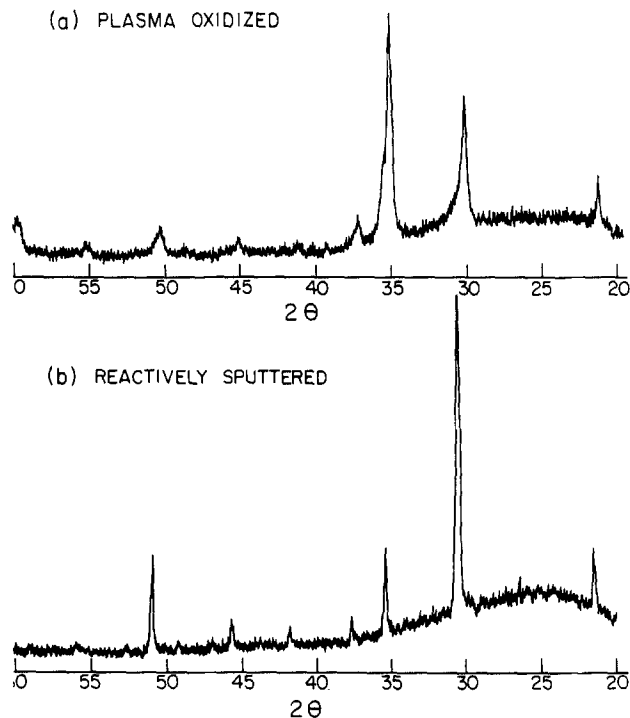


Fig. 7. XRD spectra of the (a) rough plasma grown In_2O_3 and (b) reactively sputtered In_2O_3 .

Ontario Hydro Research Division assisted in meeting the publication costs of this article.

REFERENCES

1. L. C. Schumacher, S. Mamiche-Afara, M. Leibovitch, and M. J. Dignam, *This Journal*, **135**, 3044 (1988).
2. L. C. Schumacher, S. Mamiche-Afara, and M. J. Dignam, *ibid.*, **133**, 716 (1986).
3. R. L. Sasseville, S. Mamiche-Afara, M. F. Weber, and M. J. Dignam, "Photoelectrochemical and Electrochemical Modifications of the Behavior of Sputter Prepared thin Films of TiO_2 ," in *Hydrogen Energy Progress V*, Vol. 3, pp. 1047-1054 (1984).

A Model for the Anodic Dissolution of the Zinc Electrode in the Prepassive Region

Yu-Chi Chang¹ and Geoffrey Prentice*

Department of Chemical Engineering, The Johns Hopkins University, Baltimore, Maryland 21218

The general features of slow potentiodynamic sweeps for the zinc electrode in alkaline electrolyte have been established in previous experiments (1, 2). A typical current-potential curve (1M KOH, 25°C) can be divided into four regions: an initial dissolution region, a first linear region, a second linear region, and a passive region (Fig. 1). In this work we refer to the two linear regions as prepassive. In 1N hydroxide near room temperature, the prepassive region encompasses a potential range between about -1.3 to -1.0V vs. Hg/HgO (corresponding to -1.2 to -0.9 vs. SHE); these limits vary with hydroxide concentration, temperature, and hydrodynamic conditions.

Previously, we proposed a three-step mechanism for the anodic dissolution of zinc in the initial dissolution region (3), which was similar to a model developed by Bockris *et al.* (5). From simulations based on the model we quanti-

fied the effects of mass transport on the initial reaction rate in rotating disk electrode experiments (4). Our initial dissolution model is only valid in a limited potential range near the rest potential. At higher potentials simple extrapolation of that model predicts currents that are higher than the observed current densities; therefore, in the prepassive region other processes, such as film formation, must be involved in the overall process. Based on experimental evidence generated in this investigation and in previous studies, we deduced a reaction scheme that accounts for the general features of the simulated current-potential behavior.

Experimental

Rotating disk experiments were carried out on a Pine Instrument ASR rotator with the Model AFDTI36 disk assembly and RDE 3 potentiostat. Zinc disks 0.5 cm diameter and 99.99% pure were used. The charge passed was

* Electrochemical Society Active Member.

¹ Present address: Tamkang University, Tamsui, Taiwan, China